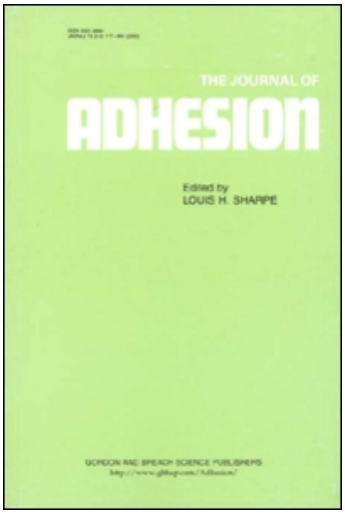

The Journal of Adhesion
Publication details, including instructions for authors and subscription information:
http://www.informaworld.com/smpp/title~content=t713453635

Surface issues of profiled cementitious composites

A. W. Momber[a]
[a] WOMA Apparatebau GmbH, Duisburg, Germany

Online publication date: 08 September 2010

To cite this Article Momber, A. W.(2002) 'Surface issues of profiled cementitious composites', The Journal of Adhesion, 78: 3, 203 — 221
To link to this Article: DOI: 10.1080/00218460210409
URL: http://dx.doi.org/10.1080/00218460210409

The Journal of Adhesion, 78: 203–221, 2002

0021-8464/02 $12.00 +.00

SURFACE ISSUES OF PROFILED CEMENTITIOUS COMPOSITES

A. W. Momber
WOMA Apparatebau GmbH, Duisburg, Germany

The paper provides a topography analysis performed on samples of hardened cement paste, mortar and concrete profiled by grit blasting. Macro-topography (profile) is evaluated by three-dimensional co-ordinate measurements, and micro-topography (roughness) is investigated via contact angle measurements. The topography of the generated surface depends on the properties of the matrix-aggregate-interface. The lower the bond, the rougher the surface. The micro-roughness of the aggregate surfaces increases due to grit blasting, but the adhesion properties, in terms of contact angle, do not necessarily improve. The contact angles depend on a balance between frictional force and capillary force and, therefore, are not a simple expression of the surface roughness.

Keywords: Contact angle; Grit blasting; Roughness; Surface profile

INTRODUCTION

Grit-blasting, as one of the oldest industrial surface treatment methods, is still a standard method in surface preparation of cementitious composites (cement matrix, mortar, concrete) prior to the application of protective coatings or concrete replacement systems. In Germany, as an example, all major regulations recommend grit-blasting for surface preparation [1–4]. Moreover, standard tests are available to estimate the resistance of concrete against this type of erosion [5].

Received 30 July 2001; in final form 27 November 2001.

The author is habilitation-fellow of the German Research Association, Bonn, at the RWTH Aachen, Department of Mining, Metallurgy and Geoscience.

The author thanks the German Research Foundation, Bonn; the RWTH Aachen, Aachen; and WOMA Apparatebau GmbH, Duisburg, Germany, for financial and administrative support. Thanks are further addressed to the Industrial Research Institute Swinburne (IRIS), and to the Swinburn University of Technology, Melbourne, Australia, for the permission to use laboratory facilities.

Address correspondence to A.W. Momber, WOMA Apparatebau GmbH, Werthauser Strasse 77-79, D47226 Duisburg, Germany. E-mail:andreas.momber@woma.de

However, simple testing in terms of mass or volume removal does not deliver any information about the surface topography that is generated.

Some studies are known dealing with the basic processes of solid particle erosion of cementitious composites. Mirza *et al.* [6] carried out investigations into the slurry erosion of various repair mortars and found that epoxy mortars are more erosion-resistant than cementitious grouts and polymer-modified cement-based mortars. This result is explained by the absence of micro pores in the epoxy matrix. More recently, Trende and Buyukoztürk [7] investigated the influence of the aggregate roughness on the interfacial bond between aggregate and hardened cement paste. These authors found that 'sandblasting' (which is actually an incorrect term since silica-containing sand is eliminated from many dry blasting applications) of granite aggregates increases the interfacial fracture energy. A transition from smooth to blasted surfaces nearly doubles the interface fracture energy. They also noticed the effect that a certain amount of air voids may be trapped in the interfacial surface as the roughness is very high. Nevertheless, the authors did not quantify the surface roughness; they just distinguished between smooth, sandblasted, and flamed. Goretta *et al.* [8] performed grit-blasting tests on a hardened cement paste and a mortar (they called this material 'concrete' in their investigation but, due to the very small aggregate size of 350 μm, it is rather a mortar) with varying impact angles and abrasive types. They found that a cement paste has a low erosion resistance at low impact angles (20°), especially if aluminium oxide is used as the blasting medium. This is explained by damping effects in the case of oblique impact. The major damage feature in the cement paste was the formation of many small cracks around the impact site. To explain this observation, the authors introduced a short-time creep because of the loss of physically bonded water in the structure due to the high temperature generated at the impact site. For the mortar, the erosion resistance increases with a drop in the impact angle. The material removal was due to a mixture of large-scale fracturing of the inclusions and smaller-scale multiple fracturing of the cement matrix. Probably, the large cracks initiated in the aggregate at high impact angle propagate into the weak interfacial zone between matrix and inclusion and promote high material removal rate. Most recently, Momber [9] found that the product of compressive strength and inclusion content is a very suitable parameter to describe the grit blasting resistance of cementitious composites.

Verhoef [10] attempted to use grit-blasting as a method to determine the resistance of rocks against abrasive wear. The author installed a so-called 'Sandblast Index' that may allow direct comparison of

grit-blasting data. Regarding the failure mechanism involved in the grit blasting of rocks, the author identified fracture along pre-existing cracks (trans-granular) within minerals or cracks along grain boundaries (inter-granular). Moreover, a fairly good relationship between the 'Sandblast Index' and the tensile strength has been found. The author also drew attention to the point that the indentation model [11] may not be applicable to pre-cracked materials since lateral rebound cracks formed during the unloading period could be stopped or branched. This effect is, in fact, observed during the solid particle erosion of some ceramics [12], and may also be considered for mortar and concrete.

The topography of grit-blasted concrete surfaces has not been yet an issue for a systematic investigation. Silverbrandt [13] published two values as well as a profile plot of a topography parameter that he called 'roughness', but he did not mention how this parameter was estimated. Randel and Wicke [14] investigated the shear-transfer of grit-blasted concrete surfaces and used the 'Sand-Section Test' as described in the section for profile evaluation. They estimated values for grit-blasted concrete surfaces of $R_t = 0.5$. Fiebrich [15] reported values between $0.2 < R_t < 0.6$. Unfortunately, these authors did not report the detailed experimental conditions.

From the point of view of treating cementitious composites as two-phase materials, consisting of a hardened cement paste as matrix and aggregate grains as inclusions, a two-level topography may be supposed. The entire surface texture may be distinguished by a parameter describing the macro-topography, called 'profile', and a parameter characterising the micro-topography, called 'roughness'. The first parameter covers cement matrix and interface, whereas the second parameter specifies the aggregate surface.

MATERIALS AND EXPERIMENTAL SET-UP

Materials and Grit-Blasting Set-up

Four different mixtures were manufactured for this investigation: two concrete mixtures, one mortar mixture, and one hardened cement paste mixture. The cement used for all mixtures was a General Purpose Cement. As fine aggregate quartz sand was used, and as coarse aggregate broken basalt was used. The maximum sand grain size was 2.8 mm, and the coarse aggregate grain size was between 5 mm and 40 mm. The grading curves of the aggregate materials followed the grading curves recommended by the ASTM Standard C 33. Basically, water-cement-ratio and aggregate content were varied. The mix compositions are listed in Table 1. The mixtures were placed in

conventional cylinder forms (15 cm in diameter and 30 cm in height). After 24 hours, the samples were released and placed under water for hardening. After 28 days, compressive strength and density as given in Table 1 were estimated from three specimens of each mixture. The compressive strength was measured with a force-controlled testing machine Type 'Avery 7112 CCG' following the Standard Specification in Reference [16]. The density was estimated as the ratio between specimen mass and specimen volume which was measured on three specimens of each mixture prior to the compressive testing. For the grit-blasting experiments, half-circular specimens, each 7 cm in height, were prepared. They were separated by a mechanical diamond saw. The weight of each specimen was estimated before (m_1) and after (m_2) the grit-blasting experiments as the average of five measurements. The accuracy of the balance used was 0.05 g. Thus, the mass loss, Δm, is given by

$$\Delta m = m_1 - m_2 \tag{1}$$

In order to evaluate the materials' resistance against grit-blasting, an erosion resistance is defined as follows:

$$R_E = \frac{\rho_M \cdot m_p}{\Delta m \cdot \rho_P}. \tag{2}$$

The erosion resistance is given in cm^3/cm^3. In the equation, ρ_M is the target material density, m_P is the grit consumption, and ρ_P is the grit bulk density. The higher the value of the erosion resistance, the more grit is required to remove a given volume from the target material. The estimated values are listed in Table 3.

For the grit-blasting tests, a conventional air-driven blasting chamber was used. The experimental conditions are listed in Table 2. The grit material was a garnet. The average grain size ($d_P = 165$ μm) was estimated as the median diameter from the grain-size distribution of the grit as shown in Figure 1. The grain shape was angular. The cross

TABLE 1 Compositions and Properties of the Investigated Materials

Mix No.	Material	Water content in kg	Cement content in kg	Sand content in kg	Aggregate content in kg	Compressive strength in MPa	Density in kg/m^3
1	mortar	202	520	1,459	–	9.1	1,871
2	concrete	171	280	841	1,019	17.2	2,016
3	concrete	180	560	609	1,019	19.8	2,168
4	paste	750	1,250	–	–	6.7	1,650

TABLE 2 Experimental Conditions

Parameter	Value
Air pressure	0.4 MPa
Nozzle diameter	8 mm
Stand-off distance	5 mm
Impact angle	90 degree
Grit type	garnet
Grit shape	angular
Grit mass flow rate	19.4 g/s
Average grit size	164 μm

section of the sample surface was divided into two parts: One part remained untouched, whereas the other part was grit-blasted. The blasting time for all experiments was $t_B = 60$ seconds.

Evaluation of the Surface Properties

The macro-topography of the surfaces, defined as 'profile' in this paper, generated due to diamond sawing and grit blasting, was evaluated by using a 3D-coordinate measuring machine Type 'FSP 529' with an accuracy of ± 10 μm in the z-direction (which is the direction of the erosion depth). The surface was scanned by a ball-shaped tip with a diameter of 2 mm. The scanning length was 80 mm in the x-direction and 20 mm in the y-direction; the scanning grid width was 1.0 mm in both directions. Thus, 2,000 points were evaluated for each surface. The z-direction was actually the dimension to be measured. As the tip touched the surface, a signal was sent to and stored in a signal processing unit. The resulting surface profile was calculated by using a standard software. The same software was utilised to calculate average profile depth, P_A, and profile depth standard deviation, S_P. The estimated values are listed in Table 3.

TABLE 3 Grit Blasting Results

Mix No.	Erosion resistance R_E in cm^3/cm^3	Sand-section test R_t in mm	Average profile depth P_A in mm	Profile standard deviation S_P in mm
1	227.5	0.80	1.55	0.47
2	233.1	0.55	1.45	0.37
3	395.6	0.31	1.38	0.27
4	287.5	0.20	0.87	0.03

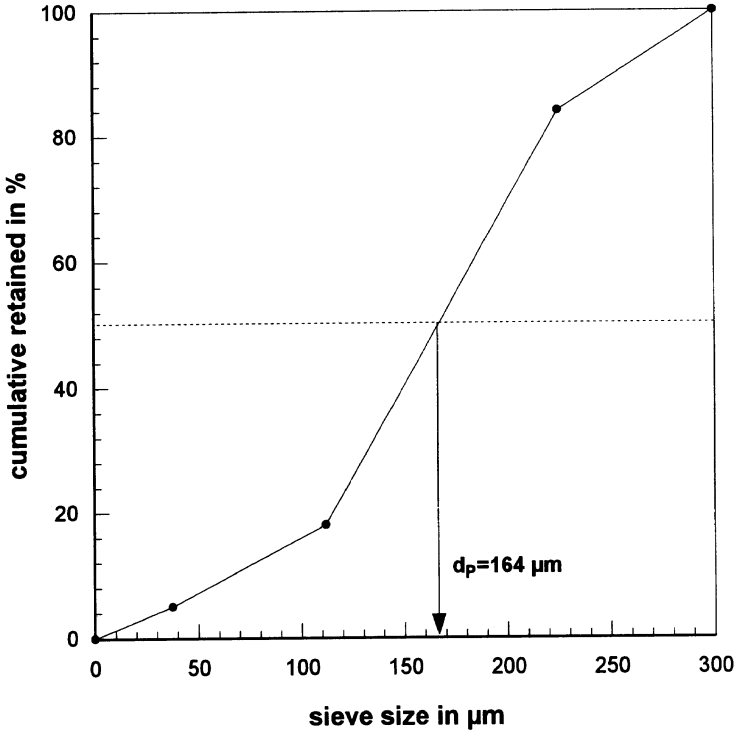

FIGURE 1 Grain-size distribution of the grit material used.

Additionally, the surface was evaluated based on the 'Sand-Section Test' as recommended in [1] and described in [1, 4]. A given volume of finely-grained garnet was applied to the specimen surface and uniformly distributed over the treated surface with a hard-wood disk. The actual evaluation parameter 'roughness depth', R_t, is given by

$$R_t = \frac{40 \cdot V}{\pi \cdot D^2} \tag{3}$$

In the equation, R_t is in mm, V is the garnet volume in cm^3, and D is the diameter of the garnet disc formed on the surface in cm. The higher the value for R_t, the higher the surface roughness. The estimated values for R_t are listed in Table 3.

The micro-topography, defined as 'roughness' in this paper, and the adhesion properties of the surfaces were indirectly evaluated by contact angle measurements. The surfaces were evaluated by using the Captive Drop Technique (CDT). The apparatus used for this procedure

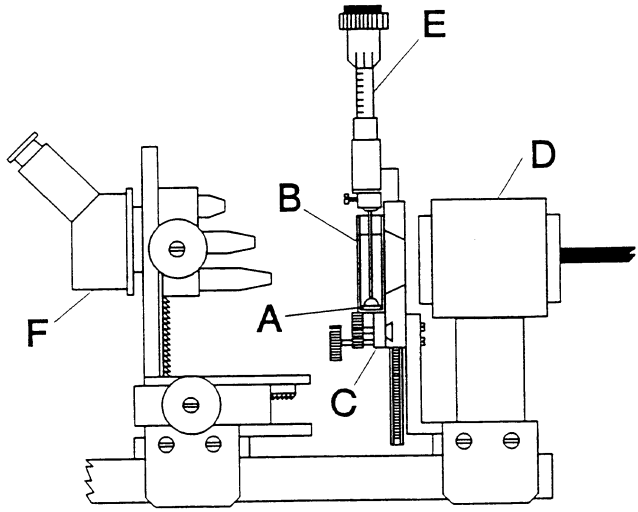

FIGURE 2 Contact angle estimation with the Captive Drop Technique (CDT).

is shown in Figure 2. It consists of a modified video microscope with an attachment for mounting a micrometer syringe. The specimen upon which a contact angle measurement was to be made (A) was placed in the thermostatted sample cell (B) on a movable platform (C) at a constant temperature. The cell was then filled with water and a liquid drop is formed at the end of the syringe and allowed to equilibrate. The contact angle was directly calculated using an FTA 200 (First Ten Angstroms) software package from an image of the drop taken with a 'Pelaco' video camera. The accuracy of the calculation is about $\pm$ 2°. Exemplary photographs obtained by this method are shown in Figure 3.

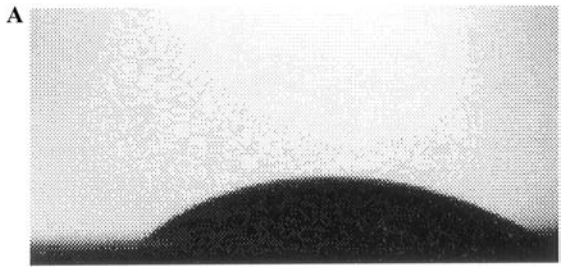

FIGURE 3 Contact angle images obtained from the CDT. (a) - Cement matrix surface, grit-blasted ($\theta = 50°$); (b) - Cement matrix surface, saw-cut ($\theta = 36°$); (c) - Concrete surface, grit-blasted ($\theta = 40°$); (d) - Aggregate in concrete, grit-blasted ($\theta = 48°$).

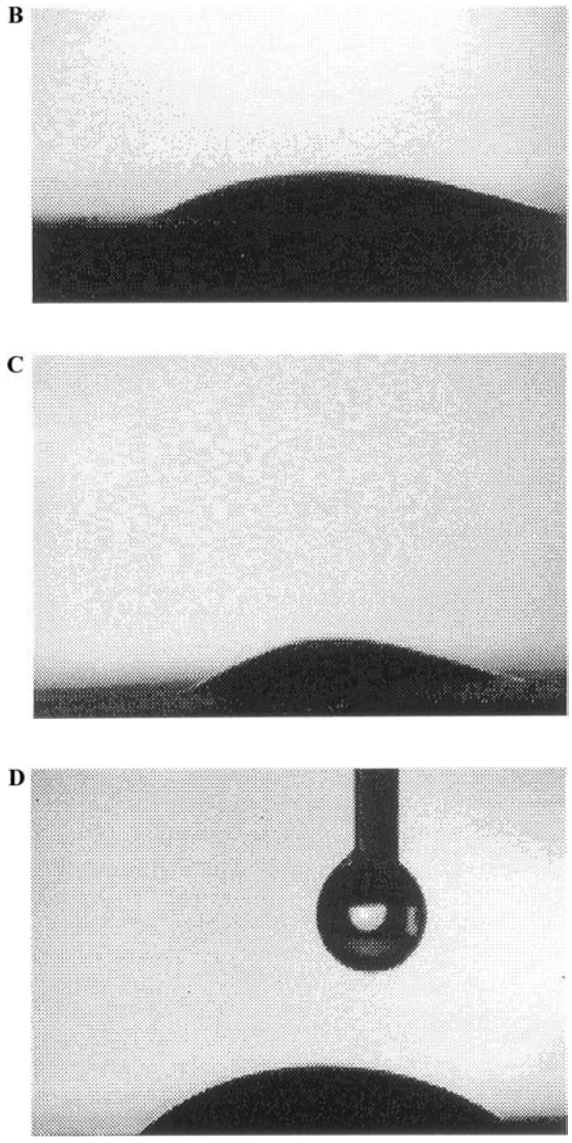

FIGURE 3 (*continued*).

RESULTS AND DISCUSSION

Macro-Topography and Surface Profile

Figure 4 exhibits the diamond saw profiles and grit-blasting profiles of the four specimens, First of all, the figures show a modification in the surface profile after the samples have been grit-blasted. Also, the striations generated during the sawing process can clearly be distinguished in each figure. Note further that any grit-blasting profile plot shows certain individual features.

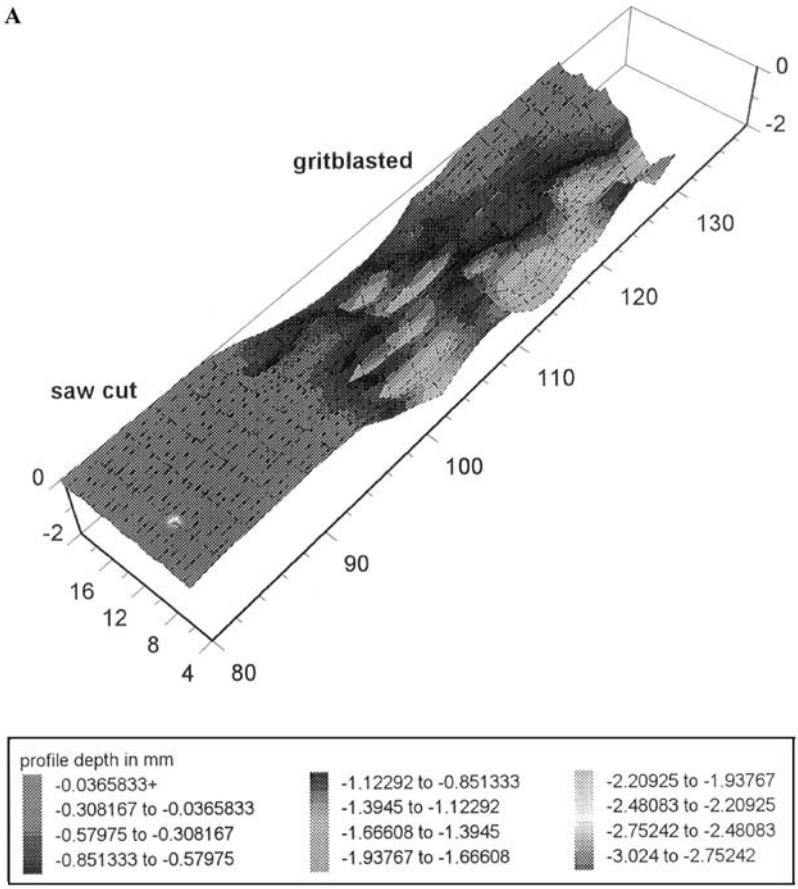

FIGURE 4 Macro-topography plots from the co-ordinate measurement machine (all dimensions in mm). (a) Mortar (mixture 1); (b) Cement matrix (mixture 4); (c) Concrete (mixture 3); (d) Concrete (mixture 2).

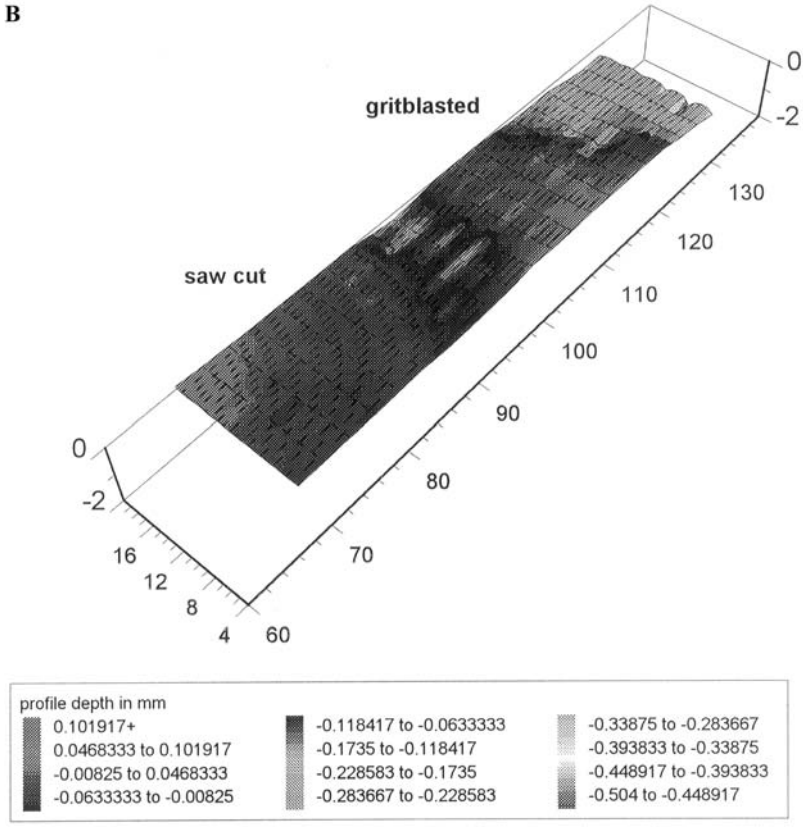

FIGURE 4 (*continued*).

The grit-blasted mortar surface (Figure 4a) has a strongly non-regular structure; areas with an accumulation of deep impressions (in the front part) alternate with areas that appear just roughened. This is also expressed by the highest standard deviation of the profile depth for this specimen (see Table 3). The accumulated impressions are up to 2 mm in depth and their length is about 10 mm. However, their micro-texture (dimensions smaller than 1 mm) shows a peak-and-valley structure. Thus, in the mortar specimen a large specific surface is generated which should benefit a good mechanical bond to the applied replacement or surface protection system. These results agree very well with the results from the sand-section test (see Table 3): The mortar has the highest value for R_t and, therefore, the roughest profile.

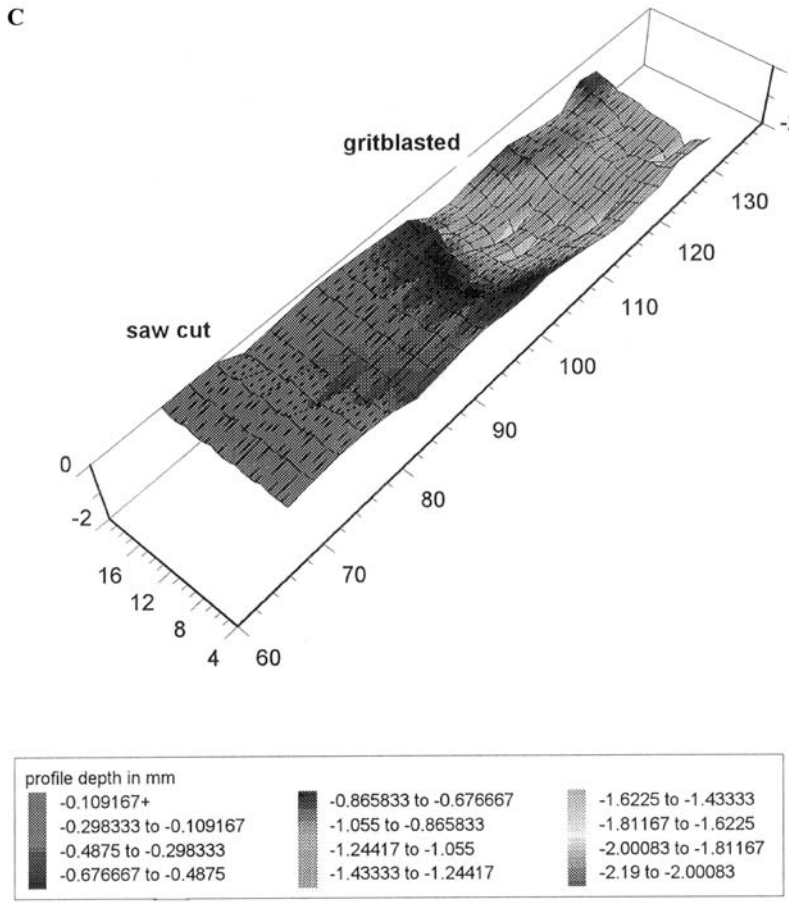

FIGURE 4 (*continued*).

The grit-blasted cement matrix (Figure 4b) shows a comparatively smooth profile. In certain regions, it even appears unaltered. However, in the transition zone between saw cut and grit blasted surface, some shallow depressions can be seen. It is found from optical inspection that these depressions occur in the immediate neighbourhood of pores. It seems that sharp pore walls are smoothed by the impact of the grit particles. Generally, there is no notable increase in the specific surface in the grit-blasted section of the specimen. Note from Table 3 that the cement mixture shows the lowest values of R_t and, therefore, the smoothest profiles which agrees with the profile measurements. It shows also the lowest standard deviation of the profile depth.

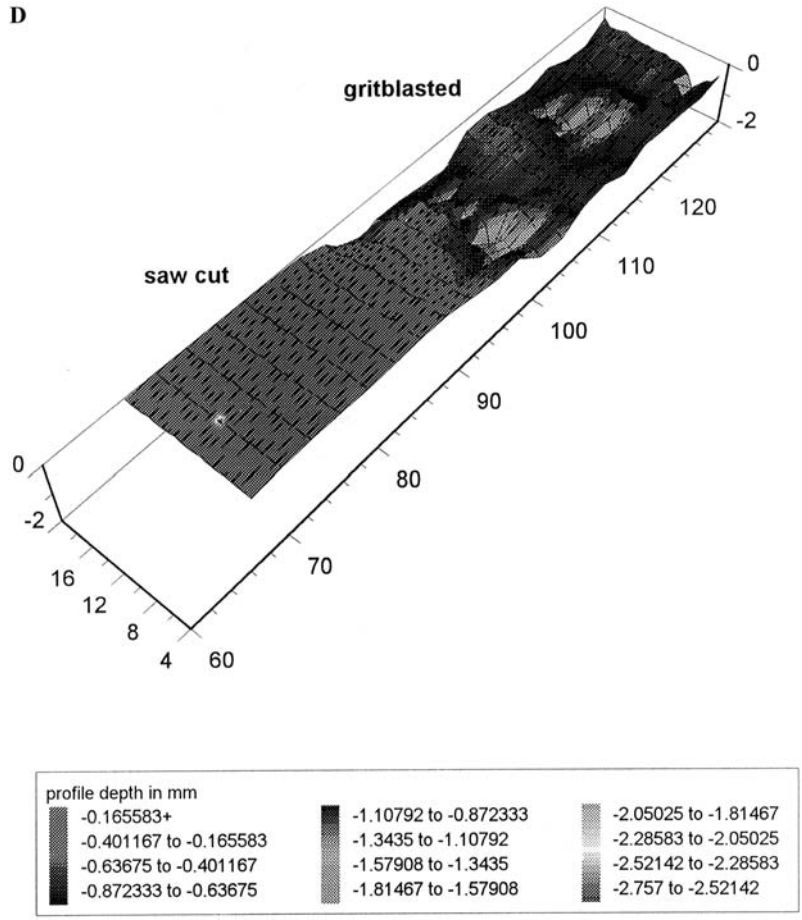

FIGURE 4 (*continued*).

Similar is the situation with the concrete mixture 3 shown in Figure 4c. Although a modification in the profile due to grit-blasting can clearly be noticed, no notable structure is generated. The generated cavities are shallow and have large dimensions. There exists no sharp transition between peaks and valleys. Again, the results from the sand-section test (Table 3) match the results from the profile measurements: The value for R_t is relatively low.

Very different are the features of the concrete mixture 2 as illustrated in Figure 4d. Here, a pronounced peak-to-valley structure can be seen. The cavities characterised by the bright spots are small and deep. Interestingly, they are concentrated in the interface between

cement matrix and aggregate. The dark peak in the rear centre position of the grit-blasted surface is actually a coarse aggregate grain. Around this grain, the matrix is removed due to the impacting abrasives. Most probably, the original interface was comparatively weak. Generally, the profile is rough and a notable increase in the specific surface occurred due to the grit-blasting process. However, the profile is not as pronounced as that of the mortar specimen. Again, the sand-section test delivers comparative results (Table 3): The R_t-value of mixture 2 lies between the values for the mortar and the concrete mixture 3.

Figure 5 shows a comparison between the results obtained from the profile measurements and the 'Sand-Section Test'. The average profile depth is that of the grit-blasted specimens sections only. A distinct relationship between the results obtained from the two experimental methods can be noticed. As average profile depth increases, roughness depth increases. Therefore, the 'Sand-Section Test' seems to be a reliable method for on-site profile evaluation of cementitious surfaces. The values for the roughness depth found in this study agree very well with results from Randel and Wicke [14]

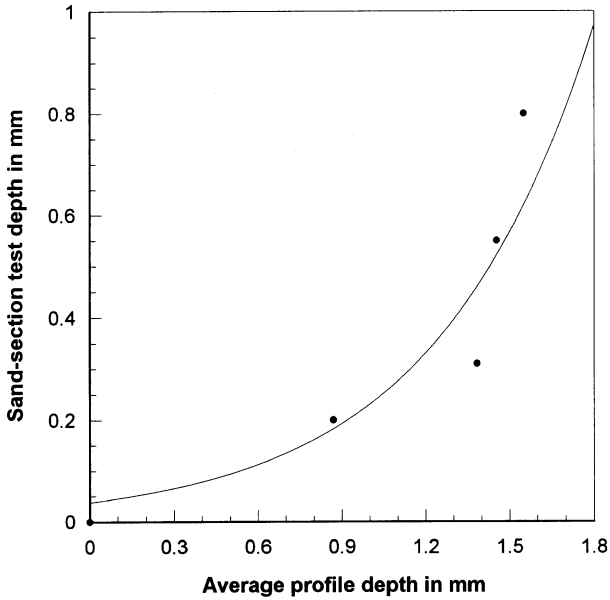

FIGURE 5 Comparison between results obtained from co-ordinate measurements and 'Sand-Section Test'.

and Fiebrich [15] who measured average values of $R_t = 0.5$ mm at grit-blasted concrete surfaces.

If the materials considered are only those that consist of matrix and aggregate inclusion, there is a distinct relationship between the profile and the erosion resistance as estimated by Eq. (2): the higher the erosion resistance, the lower the profile roughness.

Results of Contact Angle Measurements

Typical images obtained from the contact angle measurements are shown in Figure 3. There are some interesting results to be mentioned from the measurements on the cement matrix surface as shown in Figure 6a: The contact angle of the untreated surface is very high; the surface is rather hydrophobic. Basically, three types of force act against the deformation of a fluid drop applied to a solid surface: inertia forces, friction forces, and capillary forces. Considering non-porous materials, an increase in the contact angle may be the result of an increase in surface roughness according to Wenzel's formulation [17]:

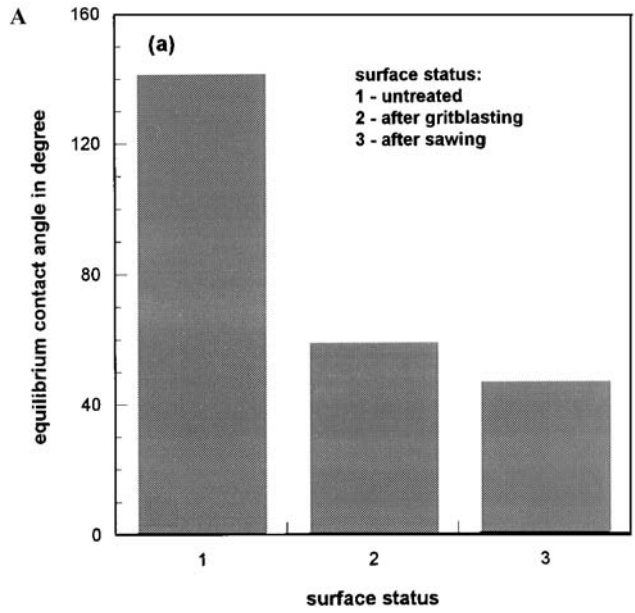

FIGURE 6 Results of contact angle measurements (each angle is the average of eleven measurements). (a) Cement matrix surfaces; (b) Concrete surfaces; (c) Aggregate (basalt) surfaces.

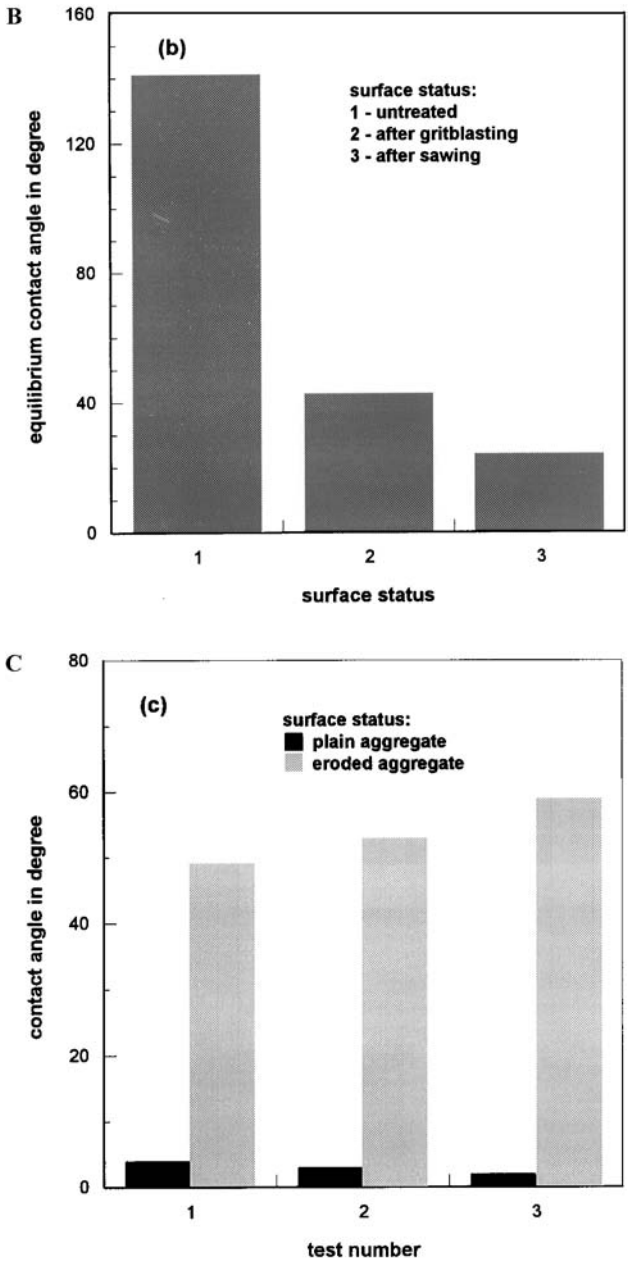

FIGURE 6 (*continued*).

$$r = \frac{\cos\theta_R}{\cos\theta} \propto \frac{A_R}{A_0} \tag{4}$$

Here, r is a so-called roughness factor considering the profile of a rough surface, θ_R is the contact angle of the rough surface, A_R is the true (rough) surface, and A_0 is a perfectly smooth surface. For a completely smooth surface, $r = 1$ and $\theta_R = \theta$. It can be seen from Eq. (4) that the contact angle increases as the roughness factor increases. It was, in fact, shown by O'Kane *et al.* [18] on orthodontic bonding cements that the contact angle increases as material surface roughness increases.

However, the materials used in this study are highly porous. If the pores are open to the surface, capillary forces may act at the water drop. If the capillary effect absorbs part of the wetting fluid in a sufficiently short period of time, contact angles increase [19].

From the latter argument, high contact angles can be concluded for the non-profiled surfaces since the external layer of any formwork-concrete surface is an accumulation of porous cement paste [4]; the capillary forces developed in the open capillary pores may reduce the radial movement of the fluid. Since the surface profile of the virgin surface ($R_t = 0.1$) is lower than that of the grit-blasted surface ($R_t = 0.2$), it can be concluded that grit-blasting does not generate a notable roughness on the virgin cement matrix surface, but only removes the porous top layer contributing to a decrease in the adhesion of fluids on the surface. A typical contact angle measured at a grit-blasted cement surface is shown in Figure 3a. However, as shown in Figure 6a, the contact angle of a saw-cut surface slightly increases after grit-blasting which points to a modification of the surface texture due to grit-blasting if the material bulk is considered. A typical contact angle measured at a saw-cut cement surface is shown in Figure 3b; note also the higher contact angle compared with Figure 3a. Therefore, grit-blasting may generate a micro-roughness at the surface of the bulk material, or it forms micro-cracks in the cement matrix surface as observed by Goretta *et al.* [8] which hinder the radial movement of the fluid. This effects may be explained by Eq. (4).

The observations are further supported in Figure 6b, showing results of comparative contact angle measurements on the concrete surfaces. Note that the contact angles for the untreated concrete surface and the contact angles for the untreated cement surface (Figure 6a) are almost equal. This is consistent with practical concreting experience: The top layer of a concrete generated in a formwork always consists of a layer of highly porous cement matrix without any aggregates. This is due to the vibrations involved in the

manufacturing process [4]. However, grit-blasting decreases the contact angle compared with the untreated surface, but this is again due to the removal of the porous top layer. Similarly to Figure 6a, grit-blasting reduces the contact angle of saw-cut surfaces (up to 60%) suggesting the modification of the microstructure of the bulk surface as already discussed. A typical contact angle measured at a grit blasted concrete surface is shown in Figure 3c.

The decrease in the contact angle due to grit-blasting is very pronounced for the mixture 1 which corresponds well with the results from the profile measurements (see Figure 4c). The contact angles given for this concrete mixture are taken from the overall surface, which includes aggregate surfaces and cement matrix surfaces as well.

The contact angles given in Figure 6c for the concrete mixture 3 are those from the aggregate surfaces only. Note that these angles are lower than the contact angles measured on the untreated surfaces shown in Figures 6a and 6b. If only the aggregate surface is considered, grit-blasting is beneficial to the contact angle. The contact angle estimated on plain aggregates is between $0^\circ < \theta < 5^\circ$; this agrees with values reported by Fiebrich [15] who found contact angles at basalt surfaces of $\theta \approx 7^\circ$. Thus, the material is rather hydrophilic. Here, grit-blasting increases the contact angle up to values between $50^\circ < \theta < 60^\circ$. A typical contact angle measured at a grit-blasted aggregate surface is shown in Figure 3d. This result may be due to two reasons. Firstly, the micro-profile of an aggregate grain may be modified by the impacting solid particles, and a micro-roughness may be formed due to large-scale fracturing of the inclusions as observed and discussed by Goretta *et al.* [8]. Secondly, micro-cracks may be generated at the material surface, hindering the radial movement of the testing fluid and increasing the contact angle. This phenomenon has been observed during the hydro-profiling of carbon steel [20]; in that study it was found that the spreading distance of a wetting fluid applied to a profiled surface reduces for comparable roughness parameters due to micro-crack formation in the target surface.

An interesting observation was made during the contact angle measurements at the saw-cut cement surfaces. It seemed that the contact angle depended on the number of grooves covered by the drop. If the drop covers more than one groove, the contact angle is between $23^\circ < \theta < 34^\circ$; if the drop covers one groove, the contact angle is between $42^\circ < \theta < 46^\circ$; if the drop does not cover any groove, the contact angle is between $57^\circ < \theta < 66^\circ$. Thus, the more grooves that are covered by the drop, the lower the contact angle. However, further investigations may be required to install a relationship between the contact angle and the location of measurement.

SUMMARY AND CONCLUSIONS

The results of this study can be summarised as follows:

- Surface topography parameters of cementitious composites profiled by grit-blasting and sawing, namely profile, roughness and contact angle, are investigated.
- The profile of a grit-blasted cement matrix surface is comparatively smooth.
- The profile of a grit-blasted mortar is very rough and non-regular.
- The profile of a grit-blasted concrete depends on the properties of the interfacial zone between cement matrix and aggregate. A weak interfacial zone promotes an irregular profile.
- Grit-blasting does not generally increase the contact angle of the generated surfaces. A simple exposure of near-surface aggregates decreases the contact angle. However, if the bulk material is considered, grit-blasting increases the contact angle compared with mechanical sawing. If the aggregate surface itself is eroded by the grit particles, the contact angle increases.
- The values for the contact angle depend on the balance between frictional force and capillary force and, therefore, are not a simple expression of the surface roughness.
- Results obtained from the 'Sand-Section Test' agree with those obtained from 3D-coordinate measurements.

REFERENCES

[1] *Zusätzliche Technische Vertragsbedingungen und Richtlinien für Schutz und Instandsetzung von Betonbauteilen* (Bundesminister für Verkehr, Verkehrsblatt-Verlag, Dortmund, 1990).
[2] *Richtline für Schutz und Instandsetzung von Betonbauteilen* (Deutscher Ausschuß für Stahlbeton, Berlin, 2001).
[3] DIN 18349 - *VOB Verdingungsordnung für Bauleistungen, Teil C: ATV Betonerhaltungsarbeiten* (Beuth-Verlag, Berlin, 2000).
[4] Momber, A.W., and Schulz, R.-R., *Betonoberfläche—Beschichtungsuntergrund: Bearbeitung, Eigenschaften, Prüfung* (Birkhäuser, Basel, 2002), to be published.
[5] Abrasion Resistance of Concrete by Sandblasting. *ASTM C 418-81* (American Society for Testing and Materials, Philadelphia, 1982).
[6] Mirza, J., Turenne, S. and Masounave, J., *Canadian J. of Civil Engrs.*, **17**, 12 (1990).
[7] Trende, U. and Buyukoztürk, O., *ACI Materials J.,* July–August, 331 (1998).
[8] Goretta, K.C., Burdt, M.L., Cuber, M.M., Perry, L.A., Singh, D., Wagh, A.S., Routbort, J.L. and Weber, W.J., *Wear*, **224**, 106 (1999).
[9] Momber, A.W., *Wear*, **246**, 46–54 (2000).
[10] Verhoef, P.N., *Int. J. Rock Mechanics Mining Science & Geomech. Abstr.*, **24**, 185 (1987).
[11] Lawn, B. and Swain, M.V., *J. Materials Sci.*, **10**, 113–122 (1975).

[12] Hutchings, I.M., *Tribology—Friction and Wear of Engineering Materials* (Edward Arnold, London, 1992).
[13] Silfwerbrand, J. and Paulsson, J., *Concrete Intern.*, **20**, Oct., 56–61. (1998).
[14] Randel, N. and Wicke, M., *Beton- und Stahlbetonbau*, **95**, 461–473 (2000).
[15] Fiebrich, F., *Kunststoffbeschichtungen auf ständig durchfeuchtetem Beton.* Deutscher Ausschuß für Stahlbeton, Heft 410 (Beuth Verlag, Berlin, 1990).
[16] Methods of Testing Concrete, Australian Standard No. 1012, Part 8 (Specification), 1975.
[17] Wenzel, R.W., *Ind. and Engng. Chem.*, **28**, 988 (1936).
[18] O'Kane, C., Oliver, R.G. and Blunden, R.E., *Brit. J. of Orthodontics*, **20**, 297 (1993).
[19] Schubert, H. *Kapillarität in porösen Feststoffsystemen* (Springer-Verlag, Berlin-Heidelberg, 1982).
[20] Momber, A.W., Wong, Y.C., Budidharma, E. and Tjo, R., *Wear*, **249**, 854 (2001).